JOURNAL OF THE ROYAL SOCIETY Interface

J. R. Soc. Interface (2005) **2**, 309–318
doi:10.1098/rsif.2005.0039
Published online 18 May 2005

Statistical geometry of pores and statistics of porous nanofibrous assemblies

Stephen J. Eichhorn† and William W. Sampson

School of Materials, University of Manchester, Manchester M60 1QD, UK

The application of theoretical models to describe the structure of the types of fibrous network produced by the electrospinning of polymers for use in tissue engineering and a number of other applications is presented. Emphasis is placed on formal analyses of the pore size distribution and porosities that one would encounter with such structures and the nature of their relationships with other structural characteristics likely to be important for the performance of nanofibrous materials. The theoretical structures considered result from interactions between randomly placed straight rods that represent fibres with nanoscale dimensions. The dominant role of fibre diameter in controlling the pore diameter of the networks is shown and we discuss the perhaps counter-intuitive finding that at a given network mass per unit area and porosity, increasing fibre diameter results in an increase in mean pore radius. Larger pores may be required for ingrowth of cells to nanofibrous networks, hence this study clarifies that simply making the diameters of the fibres smaller might not be the way to improve cell proliferation on such substrates. An extensive review of structural features of the network such as the distribution of mass, inter-fibre contacts and available surface for cell attachment, fibre contact distributions for integrity of the networks and the porosity and pore size distributions is given, with emphasis placed on nanofibre dimensions for the first time.

Keywords: porosity; electrospinning; modelling; tissue engineering

1. INTRODUCTION

There has been increasing interest over recent years in the manufacture and properties of electrospun fibrous networks for application as scaffolds in tissue engineering, filters, protective clothing, reinforcement in composite materials and sensors (Jayaraman *et al.* 2004). In particular, much emphasis has recently been placed on the need to control the diameter of nanofibres for such applications, and formal analysis of this has taken place (Fridrikh *et al.* 2003). During the electrospinning process, it is usual that a volume of polymeric solution is contacted with a large electric potential, and ultimately delivered to a needle tip where it is deformed under the electric field. This deformation is caused by the build-up and repulsion of like-charges on the surface of the solution which, if they reach a certain density, will overcome the surface tension and cause a jet to be delivered to an earthed target (Doshi & Reneker 1995). The understanding of the process itself has its roots with the work of Rayleigh (1882) who investigated the effect of an electrostatically charged object in close proximity to a liquid. Later Zeleny (1914) discovered the point of electrostatic instability of a liquid, and a form of the electrospinning process was patented by Formhals (1934). Taylor (1964, 1969) made attempts to derive in a formal mathematical sense the physics of the process at the point at which the surface tension of a liquid breaks down under electrostatic charge. Later, work by Larrondo *et al.* (1981*a–c*) into the use of polymer melts, and subsequently polymer solutions by Doshi & Reneker (1995) has subsequently led to a large body of work in this area. The materials produced by this process usually resemble fibrous networks (Doshi & Reneker 1995; Srinivasan & Reneker 1995). Although nanoscaled fibres can be produced by electrospinning, typical diameters have been reported in the range 10 μm–10 nm (Fridrikh *et al.* 2003). Circular cross-sections are also typically produced, although under certain conditions, other geometries such as tubes and collapsed tubes that result in ribbon-like structures have been reported (Koombhongse *et al.* 2001).

The production of nanofibrous networks is not exclusive to the process of electrospinning, and some recent work has investigated the similarities between carbon nanotube networks and paper (Yi *et al.* 2004). Other work has focused on the geometry of these networks and the mechanical properties achievable from such structures (Berhan, Yi & Sastry 2004; Berhan, Yi, Sastry *et al.* 2004). It is well known from the literature that the properties of stochastic fibrous networks such as paper are strongly influenced by their structure, and this work has been extensively reviewed (Deng & Dodson 1994; Sampson 2001*a*).

Conventionally, the standard reference structure for the modelling of such networks is one where

†Author for correspondence (stephen.j.eichhorn@manchester.ac.uk).

Received 30 November 2004
Accepted 18 March 2005

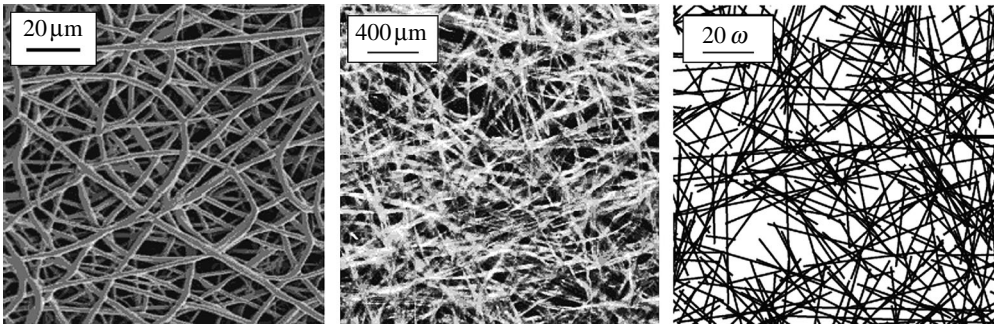

Figure 1. Images of fibrous networks for an electrospinning process (left), a paper-like material (middle) and a modelled structure (right). Scale for the modelled structure is for 20 fibre widths (20ω).

the locations of fibre centres are distributed according to a point Poisson process in two-dimensions, and hence are independent of each other. In such random fibrous networks, the orientation of the major axes of fibres to a given direction typically has a uniform distribution. This body of theory allows computation of several important structural features of random fibre networks. Here, we provide a summary of these theoretical expressions, and for the first time present their sensitivity to network and fibre variables pertinent to nanoscale structures. Two variables, with particular reference to tissue engineering, will be emphasized; namely available fibre fraction (for cell adhesion) and pore size and its distribution (for cell ingrowth). The distribution of mass will also be discussed since this has implications for the uniformity of voids in the structure. Formulae are presented as a toolbox for the reader to estimate structural characteristics of networks, and to guide the selection of experimental conditions likely to yield desirable structural characteristics such as pore size and its distribution. Importantly, we do not differentiate between the origin of the networks discussed (e.g. nanotubes or paper) and concentrate only on the issues of scale, as the class of structures is the same to a large degree, irrespective of the constituent materials.

2. BACKGROUND THEORY

There are five primary variables that influence the structural characteristics of a random fibrous network. These are often coupled to some extent, and we shall see that one of the benefits of applying statistical models to predict the influence of these variables on network structure is that they allow them to be fully decoupled in a manner not readily achievable in the laboratory.

Fibres in a network, for simplicity, can be modelled as solid straight rods characterized by three variables: length, λ, width, ω, and linear density, δ. The linear density of a fibre is defined as its mass per unit length, and is given by the product of the density of the solid from which the fibre is formed, and the cross-sectional area of the fibre. The two variables that characterize the network as a whole are its mean porosity (ε) and its mean coverage ($\bar{c}$), the latter of which is defined as the expected number of fibres covering a point in the plane of support of the network. This latter variable is extremely important since, for fibres of a given morphology, it influences the expected mass, and total fibrous length, per unit area of the network and therefore controls the extent of interaction between fibres. It is therefore an important parameter in the structural integrity of a tissue engineering scaffold. We term the mass per unit area of the network its 'areal density' and a network with mean areal density $\bar{\beta}$ has mean coverage

$$\bar{c} = \frac{\bar{\beta}\omega}{\delta}. \tag{2.1}$$

While the mean coverage can take any positive real value, the coverage at any point, c, is a discrete random variable. The probability that a point in the plane of the network has coverage c is given by the Poisson probability

$$P(c) = \frac{\bar{c}^c \mathrm{e}^{-\bar{c}}}{c!} \quad \text{for } c = 0, 1, 2, 3\ldots. \tag{2.2}$$

We note that in a network of mean coverage $\bar{c}$, the expected number of fibres in an area x^2 is given by

$$\bar{n}_\mathrm{f} = \frac{\bar{c}x^2}{\lambda\omega}. \tag{2.3}$$

It is apposite at this point to highlight the qualitative similarity between theoretical structures and those of stochastic fibrous networks that can be formed experimentally. Figure 1 shows two micrographs of experimentally realized fibre networks and graphical representation of a random fibrous network. It is important to note that all models produced here relate to analytical expressions, and numerical solutions to these where analytical forms are intractable. Therefore, we do not generate computer images, and thus the model structure shown in figure 1 is illustrative, and not for analysis. Hence, boundary conditions as described by Yi *et al.* (2004) would not apply to our approach. On first inspection it is clear that the electrospun network shown in the image on the left is qualitatively similar to that of the laboratory-formed paper sample shown in the central image and these in turn share similarities with the random network of fibres shown on the right. Interactions between fibres and other stochastic perturbations result in the structure of industrially formed stochastic networks exhibiting a greater degree of fibre clumping than is observed for random networks, though many structural characteristics are affected only locally and global average values are often

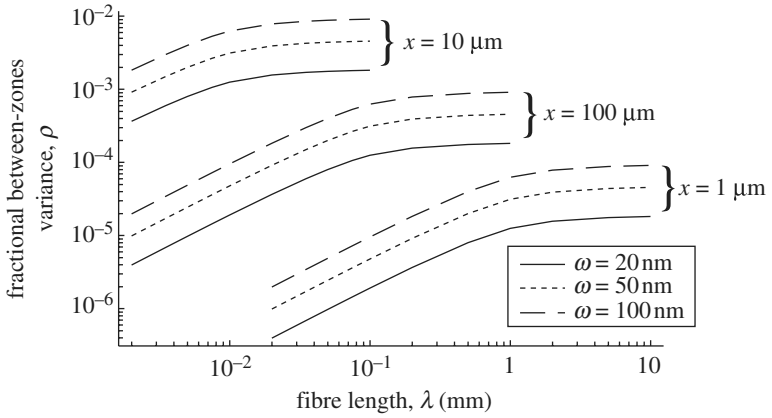

Figure 2. The fractional between zones variance, ρ plotted against fibre length for different fibre widths and scales of inspection.

unaffected (Deng & Dodson 1994; Sampson 2001*a*). In electrospinning, the network is formed effectively at the same time as the fibres, and opportunities for interactions between fibres are limited until they assume their final location in the network. As such, we expect the random model to agree more closely with the structures formed in these experiments, and note that this agrees with observations of other workers (Matthews *et al.* 2002). Models that discuss the percolation of what could be considered light networks of random straight rod constructs, such as those espoused by Balberg & Binenbaum (1983) and subsequent papers, where percolation is an issue, are not covered in our treatment. This is because our networks are so dense that we are well-above the percolation thresholds, and therefore do not require this type of analysis. In the case of electrospun networks, the fibres can be considered infinitely long, and therefore by definition percolated.

3. DISTRIBUTION OF MASS

Having discussed some preliminary definitions of the networks, we now turn to the distribution of material, and hence the void structure. Now, since the coverage is a random process, we expect its local average value to vary from region-to-region. One the most fundamental measures of network uniformity is the distribution of local average coverage in the plane, and this manifests itself as a distribution of local average areal densities. From the central limit theorem in statistics, we expect the distribution of local averages of coverage to be Gaussian. As for any stochastically structured porous material, the observed variability will depend on the scale of the observation. The parameter of scale is worthy of some discussion, eventually with reference to nano-scaled structures, but initially to paper-like materials.

If one imagines an experiment where a piece of paper is taken and is cut into four equally sized squares, and then each piece is weighed, we can calculate the mean and variance of the mass of the intact sheet. If each individual piece is then cut again equally into four pieces as before, and we now weigh all 16 squares, we find that the observed variance increases. Continued cutting in this fashion and reweighing increases the variance, and we find, therefore, that the value of this parameter depends on what we term 'the scale of inspection'; here we will use the length of the side of such squares to characterize this scale.

Expressions to calculate the variance of local coverage at all scales have been derived by Dodson (1971), and the background theory to this covered elsewhere in the literature (Deng & Dodson 1994). The maximum variance occurs when sampling is of points, and not areas, and since we have a Poisson process, this point variance is equal to the mean. At all finite scales, the variance of local coverage is less than this by a factor, ρ that is a function of fibre length, width and the scale of inspection and is known as the 'fractional between-zones variance'. Thus, the variance of local coverage at a scale of inspection x is given by

$$\sigma_x^2(\bar{c}) = \bar{c}\rho, \tag{3.1}$$

and the coefficient of variation of local coverage is

$$\mathrm{CV}_x(\bar{c}) = \sqrt{\frac{\rho}{\bar{c}}}. \tag{3.2}$$

Calculation of the fractional between-zones variance requires numerical integration of expressions that can be found elsewhere (Dodson 1971). We have calculated this parameter for the fibre geometries that we expect to be typical of stochastic nanofibrous assemblies. The influence of fibre width, length and inspection zone size are shown in figure 2. We note, with reference to figure 1, and the vast literature in the area, that electrospun fibres will have lengths much greater than the 10 mm size likely to be encountered with the largest papermaking fibres. However, it is clear that the fractional between-zones variance is strongly dependent on fibre diameter and that it increases with increasing fibre length, reaching a plateau when the fibre length is approximately five times the inspection zone size. The observed increase with increasing fibre width is very close to linear (Deng & Dodson 1994). When the fibre length is greater than $\sqrt{2}x$, the fractional between-zones variance can be found using the approximation (Sampson 2002)

$$\rho \approx 4\left(\frac{\omega}{\pi x}\right)\left(\frac{1-\sqrt{2}}{3} - \frac{x}{4\lambda} + \log(1+\sqrt{2})\right) \quad \text{for } \lambda > \sqrt{2}x, \tag{3.3}$$

such that as $\lambda \to \infty$, $\rho \approx 0.95\omega/x$. So, as a rule-of-thumb, we can estimate the fractional between-zones variance for electrospun networks as the ratio of fibre diameter to the scale of inspection and hence, from equation (3.2),

$$\mathrm{CV}_x(\tilde{c}) \approx \sqrt{\frac{\omega}{x\bar{c}}}. \tag{3.4}$$

Equation (3.4) allows us to gauge the degree of non-uniformity that we can expect to observe in electrospun networks. At a scale of inspection of 1 mm, which is close to that at which the human eye detects variability (Deng & Dodson 1994), the coefficient of variation of local coverage of a network of fibres with diameter 100 nm, when expressed as a percentage is approximately $1/\sqrt{\bar{c}}$. As such, we may arguably consider the distribution of mass of electrospun networks to be uniform at any mean coverage likely to be realized in an experiment. In what follows it will be shown also that this uniformity of mass does not manifest itself as uniformity in the void or porous structure of the network, and this has implications for the use of nanofibrous networks for tissue engineering.

A salient point to make at this juncture is that the kind of formalism employed here is required for the characterization of tissue engineering substrates made by this technique. This is because, while it is relatively easy to make qualitative judgments as to the availability of free surfaces (related to the distribution of mass), and more so about porosity, such an approach will not yield sensible data on how cells might attach and proliferate in such a scaffold. Another point to be made is that we must beware that when we perform an analysis of an electrospun network, the scale of our measurements must be carefully monitored with reference to fibre diameter to ensure a statistically meaningful sample is taken. Before considering this in more detail we consider the density of contacts between fibres, since these determine the dimensions of inter-fibre voids.

4. INTER-FIBRE CONTACTS AND AVAILABLE SURFACE

Much of the early theory describing the structure of random fibrous networks considered the special case of two-dimensional networks. Kallmes & Corte (1960) defined a two-dimensional network, with particular reference to paper as one with a mean coverage of approximately 0.5. Deng & Dodson (1994) suggested that a reasonable maximum value for the mean coverage at which a network may be considered two-dimensional is 1. When considering networks formed by the superposition of several two-dimensional structures, Sampson (2004) has recently suggested an upper limit for the mean coverage of a two-dimensional network of $\pi/2$. These differences are not of importance to the present discussion, and it is sufficient for us to consider two-dimensional networks to be those with a negligible structural component perpendicular to the plane of the network.

The mean coverage of real networks will be much greater than those of two-dimensional networks, and many of their properties can be calculated by considering structures formed from stacking layers of two-dimensional networks. Such structures are not truly three-dimensional, since fibre axes may be inclined only within a few degrees of the plane of the network, whereas in a three-dimensional network, fibre axes may take any orientation in the solid angle 2π. Here, we restrict ourselves to discussion of layered, 'planar', networks but note that recent advances in electrospinning have allowed three-dimensional fibrous networks via electrospinning (Li *et al.* 2005) and relevant theoretical description of similar structures can be found in, for example, Ogston (1958), Parkhouse & Kelly (1995), Phillipse & Kluijtmans (1999) and Dodson *et al.* (2001*a*).

We note that since the fractional open area, ε of a network of coverage, $\bar{c}$ is given by the Poisson probability that the coverage is zero, i.e. $\varepsilon = P(0) = \mathrm{e}^{-\bar{c}}$, then the mean coverage of a two-dimensional network ($\bar{c}_{2\mathrm{D}}$) can be defined in terms of its fractional open area such that $\bar{c}_{2\mathrm{D}} = \log(1/\varepsilon)$. Higher coverage networks can be modelled as stacks of such two-dimensional networks with the number of layers being given by $\bar{c}/\bar{c}_{2\mathrm{D}}$. For these networks, the fractional open area of the two-dimensional layers is extended into three dimensions, and is therefore equivalent to the porosity of the network. Note, however, that while the fractional open area of high coverage networks may still be computed as $\mathrm{e}^{-\bar{c}}$, this does not correspond to the network porosity, since networks of any realizable coverage may exhibit any porosity and these two parameters are only coupled for two-dimensional networks.

The fraction of the fibre surface in contact with other fibres in the network, and therefore related to the available surface for cells to attach, is termed the 'fractional contact area', Φ. For networks of mean coverage less than the two-dimensional coverage, Sampson (2004) gives

$$\Phi_{2\mathrm{D}} = \varepsilon\log(\varepsilon)\left(-\frac{1}{2}+\frac{2\log(\varepsilon)}{9}-\frac{\log(\varepsilon)^2}{16}+\frac{\log(\varepsilon)^3}{75}+\cdots\right), \tag{4.1}$$

and for networks whose coverage is greater than a two-dimensional coverage

$$\Phi = \left(1-\frac{2\bar{c}_{2\mathrm{D}}}{\bar{c}}\right)\Phi_{2\mathrm{D}} + \left(1-\frac{\bar{c}_{2\mathrm{D}}}{\bar{c}}\right)\Phi^*, \tag{4.2}$$

where Φ^* is given by

$$\Phi^* = 2\varepsilon(1-\varepsilon)^2\log(\varepsilon)\left(-1+\frac{\log(\varepsilon)}{4}-\frac{\log(\varepsilon)^2}{18}+\frac{\log(\varepsilon)^3}{96}-\frac{\log(\varepsilon)^4}{600}+\cdots\right), \tag{4.3}$$

and when $\bar{c} \to \infty$, $\Phi = \Phi_{2\mathrm{D}} + \Phi^*$. It follows, of course, that the fraction of the fibre surface that is not contacting other fibres, and is therefore available for surface interactions with cells is $(1-\Phi)$.

Coleman *et al.* (2003) have reported a porosity of 0.73 for laboratory-formed networks of carbon nanoropes and Smith *et al.* (2000) report porosities in

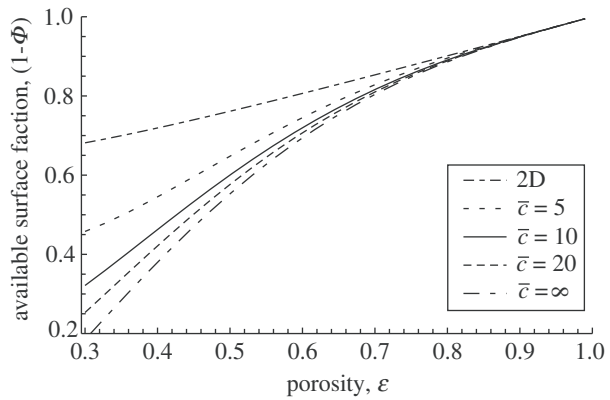

Figure 3. Available surface fraction plotted against porosity for two-dimensional networks and networks of mean coverage greater than 5.

the range 0.7–0.9 for nanotube films with an isotropic orientation of fibre axes, and 0.3 for networks where the fibres have been oriented such that preferential orientation has been set into the structure. Values for the porosity of electrospun networks, beyond qualitative statements of it being high, are difficult to find in the literature, although Kim *et al.* (2003) quote a value for silk fibroin electrospun networks of 0.76.

Equations (4.1)–(4.3) should apply to networks with arbitrary distributions of orientation, and accordingly we have plotted the available surface fraction $(1-\Phi)$ against network porosity for networks with a range of mean coverages in figure 3, using the range of porosities found in nanofibrous networks. This graph also includes a range of coverages from the two-dimensional case to an infinite value of this parameter. It can be seen that in the range of porosity for networks of nanofibres (0.7–0.9), the fraction of the surface that remains available is rather insensitive to mean coverage, although it is slightly higher for networks of low coverage, since the fibres towards the outer surfaces of the network represent a larger fraction of the total than for networks of a higher coverage. This means that care must be taken when assuming that increasing network coverage will yield greater available surface fraction at any given porosity. We note that for mean coverages greater than 10 the gradients of the curves shown in figure 3 decrease monotonically with increasing porosity, and as such, the potential to increase the availability of surface fraction through control of network porosity reduces with increasing porosity.

Discussions will now turn the distribution of fibre contacts. This has implications for the structural support of the network in tissue engineering applications, as for instance in cartilage, where the scaffold should reinforce the surrounding matrix (Svensson *et al.* 2005).

5. FIBRE CONTACTS

For two-dimensional random networks of fibres with length λ and width ω, Kallmes & Corte (1960) give the expected number of inter-fibre crossings in an area, x^2 as

$$\bar{n}_c = \frac{(\lambda \bar{n}_f)^2}{x^2 \pi}. \tag{5.1}$$

Following Kallmes & Corte (1960), Sampson (2001*a*) derived the expected number of crossings *per fibre* as

$$\bar{n}_{c,fib} = \frac{2\bar{c}_{2D}\lambda}{\pi\omega}. \tag{5.2}$$

From equation (2.3), the expected length of fibre per unit area is $\bar{c}/\omega$, so we may state that the expected number of fibre crossings per unit area in a two-dimensional network is

$$\bar{n}_{c,area} = \frac{\bar{n}_{c,fib}}{\lambda}\frac{\bar{c}_{2D}}{\omega} = \frac{2}{\pi}\left(\frac{\bar{c}_{2D}}{\omega}\right)^2. \tag{5.3}$$

Now, as discussed previously, real networks, whether they are formed by electrospinning, nanotubes or by conventional papermaking, differ from the two-dimensional structures considered by Kallmes & Corte (1960) in that they have an appreciable structural component perpendicular to the plane of the network. We also note at this juncture that fibres will not be perfectly straight, and indeed Kallmes and Corte accounted to some extent for this by the introduction of the parameter τ. This parameter scaled for the effective reduction in fibre length as a consequence of the fibre 'waviness' (Kallmes & Corte 1960) and this treatment has been refined recently by Yi *et al.* (2004). However, Yi *et al.* (2004) noted that for $\tau \sim 1$ the theory of Kallmes and Corte was adequate. Referring to figure 1, real networks can be seen to have approximately straight fibre segments. The model proposed by Yi *et al.* (2004) can accommodate much higher values of τ, and thus is well suited to the characterization of structures formed from crimped fibres such as those described by Scharcanski *et al.* (2002). Assuming that the available area for contact is $2\lambda\omega$, and noting that the expected area of a single crossing is $\pi\omega^2/2$, then it follows that the expected number of crossings per unit area in a near planar network of coverage $\bar{c}$ is

$$\bar{n}^*_{c,area} = \frac{2}{\pi}\frac{\bar{c}}{\omega^2}\Phi. \tag{5.4}$$

Now, each crossing generates a contact on each of the fibres involved, and from equation (2.3), the expected number of fibres per unit area is $\bar{c}/(\lambda\omega)$. It follows, therefore, that the expected number of contacts per fibre is

$$\bar{n}^*_{c,fib} = \frac{4}{\pi}\frac{\lambda}{\omega}\Phi, \tag{5.5}$$

and that the expected ligament length ($\bar{g}$), or the expected distance between crossings is, to a first approximation,

$$\bar{g} \approx \frac{\lambda}{\bar{n}^*_{c,fib}} - \omega \approx \left(\frac{\pi}{4\Phi} - 1\right)\omega. \tag{5.6}$$

These expressions are important because they indicate precisely what parameters influence the structural characteristics that we expect to be desirable in

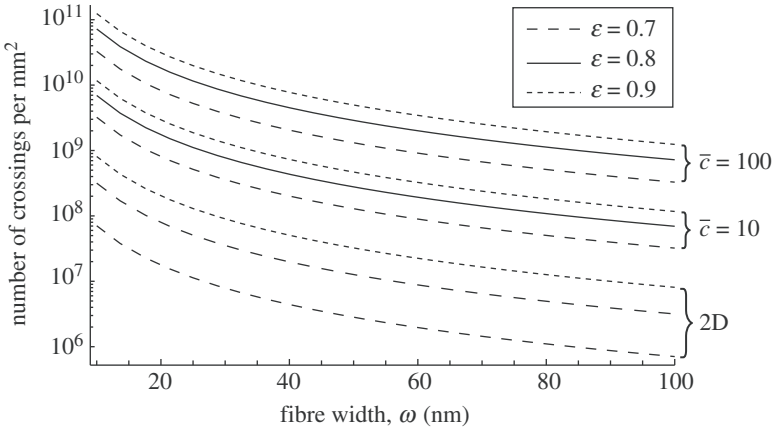

Figure 4. Number of crossings per unit area plotted against fibre width.

commercially realized networks. For example, we expect the distance between crossings to be closely coupled to the pore size distribution, and equation (5.6) tells us that the only fibre property that we expect to influence this is the fibre width (or diameter), and that the network property of interest is the fractional contact area, Φ, which we know to be influenced primarily by porosity. This means that control of fibre width is important for optimization of porosity and pore size distribution, and hence cell ingrowth into electrospun networks. The control of the diameter in electrospinning has been highlighted as a key area of investigation (Fridrikh *et al.* 2003), and perhaps a worthy experimental study would be the effect of diameter on the pore size distribution of such networks, given careful control of the mean areal density of the network.

The influence of fibre width on the expected number of fibre crossings per mm^2, as given by equation (5.4), is given in figure 4. For comparison, a family of curves giving the expected number of crossings per mm^2, as given by equation (5.3), are plotted on same axes. The porosities chosen for this plot are within the range reported by Smith *et al.* (2000), Coleman *et al.* (2003) and Kim *et al.* (2003). At mean coverages greater than approximately 10, the number of contacts per mm^2 is predictably proportional to coverage at a given fibre width and increases with decreasing fibre width. This latter observation is particularly important when considering fibres at the nanoscale, as in an electrospun network, since the sensitivity of the function increases with deceasing fibre width. Since the number of crossings per unit area is a measure of the number of ligaments per unit area, it follows that the structural integrity of a fibrous scaffolding material can only benefit from reducing the fibre width.

6. POROSITY AND PORE SIZE DISTRIBUTION

We have seen that the distribution of mass in a random fibrous network can be expressed in terms of the dimensions of the fibres, and the coverage of the network, and that, while this distribution of mass is not influenced by the mean porosity of the network, other properties, such as the number of crossings between fibres and the available fraction of the fibrous surface area, are. The distribution of porosity in the plane is of course determined by the distributions of local averages of coverage and thickness, and it has been reported that these are well described by a bivariate normal distribution (Dodson & Sampson 1999; Dodson *et al.* 2001*a*). Experimental measurements made on paper samples show that at the 1 mm scale of inspection, the coefficient of variation of density has a similar magnitude to that of coverage (Dodson *et al.* 2001*b*). Now, the coefficient of variation of coverage has been shown earlier to be low at this scale, and so we expect, therefore, that the coefficient of variation of porosity of these networks will be low also.

While the voids within a network are, by their very nature, highly interconnected and tortuous, it is often convenient to think of the network as having a distribution of pore sizes. In two-dimensional networks, pores can be considered as the polygons bounded by the segments of fibre length that occur between crossings. A study by Miles (1964) showed that the length of the sides of polygons formed from randomly generated lines has an exponential distribution, that the expected fraction of polygons that are triangles is approximately 0.36, and that the expected number of sides per polygon is four. The fraction of polygons with four sides was also shown by Miles (1964) to be approximately 0.38, and the remaining fraction can be considered to have five and seven sides. In another study, Tanner (1983) has showed that there will be few polygons in fibrous networks with more than seven sides. For a full discussion of polygons generated by a random line process in the plane, see Stoyan *et al.* (1987).

Of course the local geometry of the pores will have an effect on the spreading of cells within the nanofibrous networks used for tissue engineering. The precise distribution of polygon areas is not known analytically, but there is a growing literature that suggests that these, and the distribution of pore radii, may well be approximated by the gamma distribution (Johnston 1983, 1998; Dodson & Sampson 1996; Sampson 2001*b*), and that the standard deviation of pore radii is proportional to the mean (Bliesner 1964; Corte & Lloyd 1965; Dodson & Sampson 1996; Sampson 2001*b*). For a two-dimensional random network, of porosity

greater than about 0.3, the mean pore radius can be approximated by a function of network porosity and fibre width (Sampson 2003)

$$\bar{r}_{2D} \approx \frac{\sqrt{\pi}}{4}\left(\frac{\pi}{2\log(1/\varepsilon)} - 1\right)\omega. \tag{6.1}$$

Assuming the distribution of pore radii in the two-dimensional structure can be modelled using a gamma distribution with mean $\bar{r}_{2D} = k/b$ (where k and b are parameters that characterize the distribution) and coefficient of variation $\mathrm{CV}(r_{2D}) = 1/\sqrt{k}$, Sampson (2003) derived the probability density of pore radii in a structure formed by the superposition of n two-dimensional layers as

$$f(r) = \frac{n}{\varepsilon}\left(\frac{\Gamma(k, br)}{\Gamma(k)}\right)^{(n/\varepsilon)-1} \frac{b^k}{\Gamma(k)} r^{k-1} \mathrm{e}^{-br}, \tag{6.2}$$

where the number of layers is given by

$$n = \frac{\bar{c}}{\log(1/\varepsilon)} = \frac{\bar{\beta}\omega}{\delta\log(1/\varepsilon)}. \tag{6.3}$$

The probability density function, given by equation (6.2) itself closely resembles a gamma distribution. The mean pore radius is given by the integral

$$\bar{r} = \int_0^\infty r\, f(r)\mathrm{d}r, \tag{6.4}$$

and this must be evaluated numerically. Parameter k characterizes the uniformity of the pore radius distribution via the coefficient of variation of pore radii. While this may be affected by processing variables, here we consider it to be constant. This is because our interest is the special case of random networks and these have coefficient of variation of pore radii $\mathrm{CV}(r) = \sqrt{16 - \pi^2}/\pi$ (Corte & Lloyd 1965) and since we know k and $\bar{r}_{2D}$ from equation (6.1) we know b also.

We have computed the mean pore radius for a range of fibre morphologies and network properties that are likely to be appropriate to the study of nanofibrous assemblies. Thus, we have considered fibres of circular cross-section, with diameter up to 100 nm. The assumption of a circular cross-section permits a unique and simple relationship between diameter and linear density, which is influenced only by the density of the material from which the fibres are formed. We have assumed fibre densities between 0.9 and 1.7 g cm^{-3} to include values quoted in the literature for polycaprolactone (Koleske 1996), carbon nanotubes (Smith *et al.* 2000) and cellulose fibres (Ganster & Fink 1999). This range of values also includes most forms of polymeric materials currently used in electrospinning. The porosity range of interest here is between 0.7 and 0.9, as previously discussed. Our final parameter influencing the pore radius distribution is the mean areal density of the network. There are few studies that report this property of a nanofibrous network, although Coleman *et al.* (2003) suggest a value of about 20 g m^{-2}, and as such, we have used this as an upper limit for our calculations. We also make note that this corresponds to approximately the lower limit realized in commercial papermaking operations.

The influence of the variables of interest on the mean pore radius, calculated using equations (6.1)–(6.3) is shown in figure 5. Many of the observed behaviours are intuitively correct. For example, the mean pore size increases with increasing porosity, and decreases with increasing areal density and decreasing fibre density since these parameters influence the total fibre length per unit area in the network, and hence increase the total length of void perimeter. A less intuitive result is that at a given mean areal density and porosity, the mean pore radius increases with fibre width. This is perhaps best explained by considering two networks with the same areal density and porosity formed from fibres of different widths. As the areal density and porosity of the networks are the same, it follows that their total volumes are the same also. Denoting this volume V, we note that the volume of the networks that is occupied by fibres is $(1-\varepsilon)V$. As our networks are formed from fibres of different widths, the only way that the fibres may occupy the same volume is if the total fibre length per unit area of the thinner fibres is proportionally greater than that of the wider fibres. It is this density of fibre length per unit area that dominates the size of voids in the network. We note that, at a given coverage, increasing fibre width in a two-dimensional network will reduce the size of polygons, because the fractional open area is reduced. This should be taken into account when engineering nanofibrous networks using electrospinning techniques. The average size of a cell (Alberts *et al.* 2002), be it osteoblast, fibroblast or chondrocyte, is approximately 10 μm, and increases to 50 μm when flattened.[1] This means that *large pores* (approximately 10 μm) are required in fibrous scaffolds, unless shearing of the cells is to occur during cell migration into the network. We acknowledge that cells will have mobility (Alberts *et al.* 2002) within the network as has been seen within bacterial cellulose constructs (Svensson *et al.* 2005), but this additional component is not addressed in the present work. Additionally, we have seen that one can get different mean pore sizes for networks of the *same porosity*, and hence we must take care when making porosity measurements that we have pores large enough for cell migration. From figure 5*a* it is also clear that below 20 nm for the fibre width there is less difference in the mean pore radii of networks with porosities in the range than there is for larger fibre widths. There does, in the electrospinning community, seem to be a drive to produce ever smaller diameter fibres, with the aim of increasing surface area, but it must be emphasized that if cell proliferation into the network is desired, then the control of network porosity and mean pore radius should be decoupled.

Figure 5*b* shows how the mean pore radius (expressed in nm) increases with increasing fibre density. The scale extends to 1.7 g cm^{-3} and recent studies into using bacterial cellulose for tissue engineering (Svennsson *et al.* 2005), whose fibril dimensions are of the order of a few nanometers (Iguchi *et al.* 2000),

[1]Of course chondrocytes are usually smaller than 10 μm and do not flatten or spread in the same manner as fibroblasts or osteoblasts.

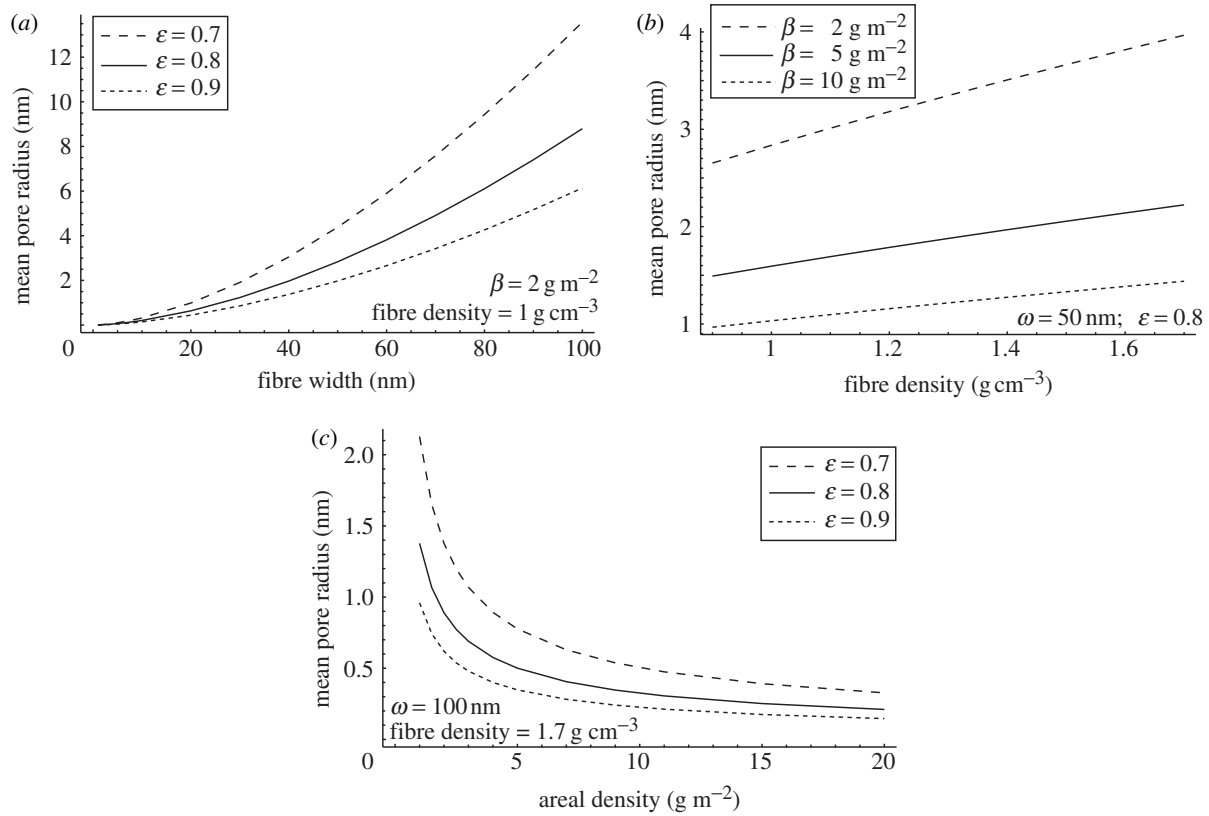

Figure 5. Influence of network and fibre variables on the mean pore radius: (*a*) influence of fibre width and porosity for constant areal density and fibre density, (*b*) influence of fibre density and areal density for constant fibre width and network porosity and (*c*) influence of areal density and porosity for constant fibre width and fibre density.

are particularly interesting with reference to this result. The density of cellulose is approximately of the order 1.5 g cm^{-3} (Ganster & Fink 1999), whereas polycaprolactone is of the order 0.9 g cm^{-3} (Koleske 1996). As one can see from figure 5*b*, this difference in density produces a dramatic difference in mean pore size, and hence the choice of material for fibrous scaffolds, particularly at the nanoscale, is of importance.

Figure 5*c* also highlights a possible risk when producing electrospun networks. Typically, the process involves spinning fibres onto a fixed target (Doshi & Reneker 1995; Fridrikh *et al.* 2003 and others). This repeated deposition over time can only increase the areal density of the network, and therefore rapidly decrease the mean pore radius. This may seem intuitive, but it is a point that has thus far not been addressed in the literature.

7. CONCLUSIONS

Much work in the area of tissue engineering, and the possibility of using nanostructured networks of fibres for composite manufacture, has been reported in the literature. However, in the former case, the need for a proper understanding of the geometry and structure of the pores within the networks is required, if optimized cell-culturing is to be obtained. Here, we have reported on the use of theoretical models to describe the structures of the types of fibrous networks produced by electrospinning and other techniques. Qualitatively, it has been shown that electrospun networks have a similar structure to fibrous networks formed by papermaking, although we suggest that the random models used as a *reference* for such structures should agree better with the former. With this in mind, we have shown that especially at the nanoscale of fibre width, a number of key issues arise. In terms of the distribution of mass, it is clear that a uniformity in this parameter does not manifest itself in the void or porous structure, and that this is strongly dependant on fibre diameter. This means that any control of fibre diameter must be done with due care to address its effect on the pore structure, and obviously and ultimately the ingress and growth of cells. It has been shown that at the nanoscale it is important that the correct inspection sizes are used for analysis of pore size and distribution, since this also depends on fibre diameter, so that statistically meaningful data is obtained. The nature of electrospun networks, in terms of their two-dimensionality has been reported. It has been shown that care must be taken when assuming that by increasing network coverage, this will in turn increase available surface area, since this is shown to be rather insensitive at the nanoscale. In terms of the fibre contacts, such a region is deemed to be a prohibited contact point for a potential cell, and hence the distribution of fibre contacts is introduced as an important parameter in fibrous networks for tissue engineering. The sensitivity of the number of fibre contacts per unit area has been shown to be proportional to coverage, and more importantly, increases with decreasing fibre width. This means that this

parameter can be clearly engineered through fibre-width control. Structural integrity of the network, particularly useful for applications where the tissue engineering scaffold may provide mechanical support, also increases with decreasing fibre width and this may be one advantage of electrospinning. However, a salient point to be derived from this work is that the mean pore radius increases with fibre width, and it may be this, and not porosity, that is desirable for such substrates.

This work has been funded by the EPSRC (grant no. EP/C004930/1). The authors wish to thank Dr Chris Wilkins for the light microscopy images of the paper samples and Nicholas Fry (Smith and Nephew) for use of the electrospun network image.

REFERENCES

Alberts, B., Johnson, A., Lewis, J., Raff, M., Roberts, K. & Walter, P. 2002 *Molecular biology of the cell*, 4th edn. New York: Garland Science.

Balberg, I. & Binenbaum, N. 1983 The percolation threshold in a two-dimensional anisotropic system of conducting sticks. *Phys. Rev. B* **28**, 3799–3812.

Berhan, L., Yi, Y. B. & Sastry, A. M. 2004 Effect of nanorope waviness on the effective moduli of nanotube sheets. *J. Appl. Phys.* **95**, 5027–5034.

Berhan, L., Yi, Y. B., Sastry, A. M., Munoz, E., Selvidge, M. & Baughman, R. 2004 Mechanical properties of nanotube sheets: alterations in joint morphology and achievable moduli in manufacturable materials. *J. Appl. Phys.* **95**, 4335–4345.

Bliesner, W. C. 1964 A study of the porous structure of fibrous sheets using permeability techniques. *Tappi J.* **47**, 392–400.

Coleman, J. N. *et al.* 2003 Improving the mechanical properties of single walled carbon nanotube sheets by intercalation of polymeric adhesives. *Appl. Phys. Lett.* **82**, 1682–1684.

Corte, H. K. & Lloyd, E. H. 1965 Fluid flow through paper and sheet structure. In *Consolidation of the Paper Web, Transactions of the Third Fundamental Research Symposium, Cambridge* (ed. F. Bolam), pp. 981–1009. Manchester: FRC.

Deng, M. & Dodson, C. T. J. 1994 *Paper: an engineered stochastic structure*. Atlanta: Tappi Press.

Dodson, C. T. J. 1971 Spatial variability and the theory of sampling in random fibrous networks. *J. R. Stat. Soc.* **33**, 88–94.

Dodson, C. T. J. & Sampson, W. W. 1996 The effect of paper formation and grammage on its pore size distribution. *J. Pulp Pap. Sci.* **22**, 165–169.

Dodson, C. T. J. & Sampson, W. W. 1999 Spatial statistics of stochastic fibre networks. *J. Stat. Phys.* **96**, 447–458.

Dodson, C. T. J., Oba, Y. & Sampson, W. W. 2001*a* Bivariate normal thickness-density structure in real near-planar stochastic fibrous networks. *J. Stat. Phys.* **102**, 345–353.

Dodson, C. T. J., Oba, Y. & Sampson, W. W. 2001*b* On the distributions of mass, thickness and density in paper. *Appita J.* **54**, 385–389.

Doshi, J. & Reneker, D. H. 1995 Electrospinning process and applications of electrospun fibres. *J. Electrostat.* **35**, 151–160.

Formhals, A. 1934 Process and apparatus for preparing artificial threads. US Patent no. 1,975,504.

Fridrikh, S. V., Yu, J. H., Brenner, M. P. & Rutledge, G. C. 2003 Controlling the fibre diameter during electrospinning. *Phys. Rev. Lett.* **90**, 1–4.

Ganster, J. & Fink, H.-P. 1999 Physical constants of cellulose. In *Polymer handbook* (ed. E. H. Immergut & E. A. Grulke) 4th edn. New York: Wiley.

Iguchi, M., Yamanaka, S. & Budhiono, A. 2000 Bacterial cellulose—a masterpiece of nature's arts. *J. Mater. Sci.* **35**, 261–270.

Jayaraman, K., Kotaki, M., Zhang, Y. Z., Mo, X. M. & Ramamkrishna, S. 2004 Recent advances in polymer nanofibres. *J. Nanosci. Nanotechnol.* **4**, 52–65.

Johnston, P. R. 1983 The most probable pore size distribution in fluid filter media. *J. Test. Eval.* **11**, 117–121.

Johnston, P. R. 1998 Revisiting the most probable pore size distribution in filter media. The gamma distribution. *Filtn. Sep.* **35**, 287–292.

Kallmes, O. & Corte, H. 1960 The structure of paper. I. The statistical geometry of an ideal two-dimensional fibre network. *Tappi J.* **43**, 737–752. (See also *Errata* 1961 **44**, 448.)

Kim, S. H., Nam, Y. S., Lee, T. S. & Park, W. H. 2003 Silk fibroin nanofiber. Electrospinning, properties and structure. *Polym. J.* **35**, 185–190.

Koleske, J. V. 1996 Poly(ε-caprolactone)—overview. In *Polymeric materials encyclopedia* (ed. J. C. Salamone), vol. 8. Boca Raton, FL: CRC Press.

Koombhongse, S., Liu, W. & Reneker, D. H. 2001 Flat polymer ribbons and other shapes by electrospinning. *J. Polym. Sci. B* **39**, 2598–2606.

Larrondo, L. & Manley, R. St. J. 1981*a* Electrostatic fibre spinning from polymer melts. I. Experimental observations on fibre formation and properties. *J. Polym. Sci.: Polym. Phys. Edn* **19**, 909–920.

Larrondo, L. & Manley, R. St. J. 1981*b* Electrostatic fibre spinning from polymer melts. II. Examination of the flow field in an electrically driven jet. *J. Polym. Sci.: Polym. Phys. Edn* **19**, 921–932.

Larrondo, L. & Manley, R. St. J. 1981*c* Electrostatic fibre spinning from polymer melts. III. Electrostatic deformation of a pendant drop of polymer melt. *J. Polym. Sci.: Polym. Phys. Edn* **19**, 933–940.

Li, W.-J., Tuli, R., Okafor, C., Derfoul, A., Danielson, K. G., Hall, D. J. & Tuan, R. S. 2005 A three-dimensional nanofibrous scaffold for cartilage tissue engineering using human mesenchymal stem cells. *Biomaterials* **26**, 599–609.

Matthews, J. A., Wnek, G. E., Simpson, D. G. & Bowlin, G. L. 2002 Electrospinning of collagen nanofibres. *Biomacromolecules* **3**, 232–238.

Miles, R. E. 1964 Random polygons determined by random lines in a plane. *Proc. Natl Acad. Sci.* **52**, 901–907. (See also pp. 1157–1160.)

Ogston, A. G. 1958 The spaces in a uniform random suspension of fibres. *Trans. Farad. Soc.* **54**, 1754–1757.

Parkhouse, J. G. & Kelly, A. 1995 The random packing of fibres in three dimensions. *Proc. R. Soc. A* **451**, 737–746.

Phillipse, A. P. & Kluijtmans, S. G. J. M. 1999 Sphere caging by a random fibre network. *Physica A* **274**, 516–524.

Rayleigh, Lord 1882 On the equilibrium of liquid conducting masses charged with electricity. *Phil. Mag. J.* **44**, 184–186.

Sampson, W. W. 2001*a* The structural characterisation of fibre networks in papermaking processes—a review. In *The Science of Papermaking, Transactions of the XIIth Fundamental Research Symposium* (ed. C. F. Baker), pp. 1205–1288. Manchester: Pulp and Paper Fundamental Research Society.

Sampson, W. W. 2001*b* Comments on the pore radius distribution in near-planar stochastic fibrous networks. *J. Mater. Sci.* **36**, 5131–5135.

Sampson, W. W. 2002 The determination of the variance of local grammage in random fibre networks by the line method. *J. Pulp Pap. Sci.* **28**, 259–261.

Sampson, W. W. 2003 A multiplanar model for the pore radius distribution in isotropic near-planar stochastic fibre networks. *J. Mater. Sci.* **38**, 1617–1622.

Sampson, W. W. 2004 A model for fibre contact in planar random fibre networks. *J. Mater. Sci.* **39**, 2775–2781.

Scharcanski, J., Dodson, C. T. J. & Clarke, R. T. 2002 Simulating the effects of fibre crimp, flocculation, density and orientation on structure statistics of stochastic fibre networks. *Simul. Trans. Soc. Model. Simul. Int.* **78**, 389–395.

Smith, B. W., Benes, Z., Luzzi, D. E., Fischer, J. E., Waltyers, D. A., Casavant, M. J., Schmidt, J. & Smalley, R. E. 2000 Structural anisotropy of magnetically aligned single wall carbon nanotubes films. *Appl. Phys. Lett.* **77**, 663–665.

Srinivasan, G. & Reneker, D. H. 1995 Structure and morphology of small-diameter electrospun aramid fibres. *Polym. Int.* **36**, 195–201.

Stoyan, D., Kendall, W. S. & Mecke, J. 1987 *Stochastic geometry and its applications. Probability and mathematical statistics*. Berlin: Wiley.

Svensson, A., Nicklasson, E., Harrah, T., Panilaitis, B., Kaplan, D. L., Brittberg, M. & Gatenholm, P. 2005 Bacterial cellulose as a potential scaffold for tissue engineering of cartilage. *Biomaterials* **26**, 419–431.

Tanner, J. C. 1983 The proportion of quadrilaterals formed by random lines in a plane. *J. Appl. Probab.* **20**, 400–404.

Taylor, G. I. 1964 Disintegration of water drops in an electric field. *Proc. R. Soc. A* **280**, 383–397.

Taylor, G. I. 1969 Electrically driven jets. *Proc. R. Soc. A* **313**, 453–475.

Yi, Y. B., Berhan, L. & Sastry, A. M. 2004 Statistical geometry of random fibrous networks revisited: waviness, dimensionality, and percolation. *J. Appl. Phys.* **96**, 1318–1327.

Zeleny, J. 1914 The electrical discharge from liquid points, and a hydrostatic method of measuring the electric intensity at their surfaces. *Phys. Rev.* **3**, 69–91.